



**Calhoun: The NPS Institutional Archive**  
**DSpace Repository**

---

Theses and Dissertations

1. Thesis and Dissertation Collection, all items

---

2009-06

**Visible-to-SWIR Downconversion and its  
application to Individual Identification Friend  
or Foe (IIFF)**

**Gardner, Scott R.**

Monterey, California. Naval Postgraduate School

---

<http://hdl.handle.net/10945/4715>

*Downloaded from NPS Archive: Calhoun*



Calhoun is a project of the Dudley Knox Library at NPS, furthering the precepts and goals of open government and government transparency. All information contained herein has been approved for release by the NPS Public Affairs Officer.

**Dudley Knox Library / Naval Postgraduate School**  
**411 Dyer Road / 1 University Circle**  
**Monterey, California USA 93943**

<http://www.nps.edu/library>



**NAVAL  
POSTGRADUATE  
SCHOOL**

**MONTEREY, CALIFORNIA**

**THESIS**

**VISIBLE-TO-SWIR DOWNCONVERSION AND ITS  
APPLICATION TO INDIVIDUAL IDENTIFICATION FRIEND  
OR FOE (IIFF)**

by

Scott R. Gardner

June 2009

Thesis Advisor:

Nancy M. Haegel

Second Reader:

Peter P. Crooker

**Approved for public release; distribution is unlimited**

THIS PAGE INTENTIONALLY LEFT BLANK

REPORT DOCUMENTATION PAGE		Form Approved OMB No. 0704-0188	
Public reporting burden for this collection of information is estimated to average 1 hour per response, including the time for reviewing instruction, searching existing data sources, gathering and maintaining the data needed, and completing and reviewing the collection of information. Send comments regarding this burden estimate or any other aspect of this collection of information, including suggestions for reducing this burden, to Washington headquarters Services, Directorate for Information Operations and Reports, 1215 Jefferson Davis Highway, Suite 1204, Arlington, VA 22202-4302, and to the Office of Management and Budget, Paperwork Reduction Project (0704-0188) Washington DC 20503.			
1. AGENCY USE ONLY (Leave blank)	2. REPORT DATE June 2009	3. REPORT TYPE AND DATES COVERED Master's Thesis	
4. TITLE AND SUBTITLE Visible-to-SWIR Downconversion and Its Application to Individual Identification Friend or Foe (IIFP)		5. FUNDING NUMBERS	
6. AUTHOR(S) Gardner, Scott R		8. PERFORMING ORGANIZATION REPORT NUMBER	
7. PERFORMING ORGANIZATION NAME(S) AND ADDRESS(ES) Naval Postgraduate School Monterey, CA 93943-5000		10. SPONSORING/MONITORING AGENCY REPORT NUMBER	
9. SPONSORING/MONITORING AGENCY NAME(S) AND ADDRESS(ES) N/A		11. SUPPLEMENTARY NOTES The views expressed in this thesis are those of the author and do not reflect the official policy or position of the Department of Defense or the U.S. Government.	
12a. DISTRIBUTION / AVAILABILITY STATEMENT Approved for Public Release; Distribution is Unlimited		12b. DISTRIBUTION CODE	
13. ABSTRACT (maximum 200 words)			
<p>The objective of this research was to demonstrate the extension of the current design of the Individual Identification Friend or Foe (IIFP) patch, to provide a response in the shortwave infrared (SWIR) region of the electromagnetic spectrum. The purpose of the IIFP patch is to mitigate fratricide during ground engagements, by emitting a near infrared (NIR) signal, when the wearer is illuminated by a targeting laser attached to the shooter's weapon. Due to the proliferation of NIR Night Vision Devices (NVDs), it is desirable to produce a version of the patch that emits in the SWIR spectrum, making its response visible to operators with next-generation NVDs, while being invisible to conventional NVDs. This further enhances the "covert" nature of the IIFP patch.</p> <p>To produce SWIR output, a visible-light emitter is used in conjunction with a downconverting phosphor filter. This thesis develops and evaluates candidates for visible-light emitters and downconverting phosphor filters in order to determine the most suitable candidate for use in the IIFP patch.</p> <p>Three potential candidate materials, based on neodymium and ytterbium phosphors, were evaluated using photoluminescence excitation spectroscopy. A quantitative comparison of the combined efficiency was performed to select an initial optimized combination. SWIR emission was observed through an InGaAs imaging array.</p>			
14. SUBJECT TERMS SWIR, visible light, fratricide, phosphor downconversion, IFF, photoluminescence excitation			15. NUMBER OF PAGES 61
			16. PRICE CODE
17. SECURITY CLASSIFICATION OF REPORT Unclassified	18. SECURITY CLASSIFICATION OF THIS PAGE Unclassified	19. SECURITY CLASSIFICATION OF ABSTRACT Unclassified	20. LIMITATION OF ABSTRACT UU

THIS PAGE INTENTIONALLY LEFT BLANK

Approved for public release; distribution is unlimited

VISIBLE-TO-SWIR DOWNCONVERSION AND ITS APPLICATION TO  
INDIVIDUAL IDENTIFICATION FRIEND OR FOE (IIFF)

Scott R. Gardner  
Lieutenant Commander, United States Navy  
B.S., University of Texas at Arlington, 1994

Submitted in partial fulfillment of the  
requirements for the degree of

MASTER OF SCIENCE IN APPLIED PHYSICS

from the

NAVAL POSTGRADUATE SCHOOL  
June 2009

Author: Scott R. Gardner

Approved by: Nancy M. Haegel  
Thesis Advisor

Peter P. Crooker  
Second Reader

James Luscombe  
Chairman, Department of Physics

THIS PAGE INTENTIONALLY LEFT BLANK

## ABSTRACT

The objective of this research was to demonstrate the extension of the current design of the Individual Identification Friend or Foe (IIFF) patch, to provide a response in the shortwave infrared (SWIR) region of the electromagnetic spectrum. The purpose of the IIFF patch is to mitigate fratricide during ground engagements, by emitting a near infrared (NIR) signal when the wearer is illuminated by a targeting laser attached to the shooter's weapon. Due to the proliferation of NIR Night Vision Devices (NVDs), it is desirable to produce a version of the patch that emits in the SWIR spectrum, making its response visible to operators with next-generation NVDs, while being invisible to conventional NVDs. This further enhances the "covert" nature of the IIFF patch.

To produce SWIR output, a visible-light emitter is used in conjunction with a downconverting phosphor filter. This thesis develops and evaluates candidates for visible-light emitters and downconverting phosphor filters in order to determine the most suitable candidate for use in the IIFF patch.

Three potential candidate materials, based on neodymium and ytterbium phosphors, were evaluated using photoluminescence excitation spectroscopy. A quantitative comparison of the combined efficiency was performed to select an initial optimized combination. SWIR emission was observed through an InGaAs imaging array.



THIS PAGE INTENTIONALLY LEFT BLANK

## TABLE OF CONTENTS

I.	INTRODUCTION .....	1
A.	BACKGROUND .....	1
B.	FRATRICIDE MITIGATION TECHNOLOGIES .....	2
1.	Glint Tape/GloTape® .....	2
2.	Infrared Beacons .....	4
3.	Individual Identification Friend or Foe (IIFF) .....	5
C.	NIGHT VISION DEVICE PROLIFERATION AND SWIR .....	7
II.	DOWNCONVERTING PHOSPHOR FILTERS .....	9
A.	BACKGROUND/CONSIDERATIONS .....	9
B.	PHOTOLUMINESCENCE EXCITATION SPECTROSCOPY .....	10
1.	SWIR06 .....	15
2.	SWIR07 .....	21
3.	SWIR09 .....	26
C.	SWIR EMISSION SPECTRA .....	28
1.	SWIR06 .....	29
2.	SWIR07 .....	30
3.	SWIR09 .....	32
III.	POLYMER LIGHT-EMITTING DIODES .....	33
A.	RED EMITTER .....	33
1.	Visible Light Spectra .....	33
B.	YELLOW EMITTER .....	35
IV.	COMBINED EFFECTIVENESS OF PLED/SWIR COMBINATION .....	37
V.	CONCLUSION .....	39
A.	VIDEO RECORDING OF SWIR EMISSION .....	39
B.	FURTHER RESEARCH .....	41
	LIST OF REFERENCES .....	43
	INITIAL DISTRIBUTION LIST .....	45

THIS PAGE INTENTIONALLY LEFT BLANK

## LIST OF FIGURES

Figure 1.	Infrared retro-reflective patches with U.S. markings (Night Vision Systems).....	3
Figure 2.	Wearable infrared beacon (Powerflare, Inc.).....	4
Figure 3.	Individual Identification Friend or Foe (IIFF) patch.....	5
Figure 4.	Responsivity of current-generation NVDs as a function of incident wavelength [From 2].....	8
Figure 5.	Visible Spectra of red and yellow PLED visible emitters.....	9
Figure 6.	PLE Experimental setup.....	13
Figure 7.	Energy level diagram for $\text{Nd}^{3+}$ (energies in $10^4 \text{ cm}^{-1}$ ) [From 4] .....	16
Figure 8.	PLE spectra (output as a function of excitation wavelength) showing effect of different substrate materials on SWIR output.....	17
Figure 9.	PLE spectra showing effect of illumination direction on SWIR output.....	18
Figure 10.	PLE spectra showing effect of pigment layer thickness on SWIR output. Estimated thicknesses are: red - 20 $\mu\text{m}$ , green - 25 $\mu\text{m}$ , blue - 30 $\mu\text{m}$ .....	19
Figure 11.	PLE showing improved response from thicker pigment layers compared to best sample from first batch (B-SWIR06-4S).....	20
Figure 12.	Energy level diagram for $\text{Yb}^{3+}$ [From 5] .....	21
Figure 13.	PLE response curve of SWIR07 $\text{Yb}^{3+}$ -based phosphor pigment.....	22
Figure 14.	PLE spectra showing effect of pigment layer thickness on SWIR emission.....	23
Figure 15.	PLE spectra showing effect of direction of incident illumination on SWIR emission.....	24
Figure 16.	PLE spectra showing improved response from thicker pigment layers compared to best sample from first batch (B-SWIR07-4P).....	25
Figure 17.	PLE spectra showing effect of various substrates on SWIR emission.....	26
Figure 18.	PLE results for three SWIR09 samples, with best SWIR06 sample (B-SWIR06-4S) shown for comparison.....	27
Figure 19.	SWIR emission from SWIR06 phosphor excited by 640 nm light.....	29
Figure 20.	SWIR emission from SWIR07 phosphor excited by 592 nm light.....	31

Figure 21. SWIR emission from SWIR07 phosphor excited by 758 nm light.....31

Figure 22. SWIR emission from SWIR09 phosphor excited by 640 nm light.....32

Figure 23. Visible emission spectra of "red" and "yellow" PLED spectra.....34

Figure 24. Still frame showing image of SWIR06 phosphor excited with yellow PLED. Recorded with InGaAs camera at a distance of 20 meters.....40

## LIST OF TABLES

Table 1.	Calculated SWIR output from emitter/phosphor combinations, both in terms of total SWIR output and SWIR output at wavelengths greater than 1 $\mu\text{m}$ .....	38
----------	-----------------------------------------------------------------------------------------------------------------------------------------------------------------	----

THIS PAGE INTENTIONALLY LEFT BLANK

## ACKNOWLEDGMENTS

This work was supported in part by a contract from the Rapid Reaction Technology Office of the Office of the Secretary of Defense, DDR&E, with further support from SOCOM Special Operations Acquisition and Logistics-Advanced Technology (SOAL-T).

I would like to thank Matt Wilkinson, Devin MacKenzie and Yuka Yoshioka of Add-Vision, Inc. for the PLED and phosphor samples that were the basis for all of my experimental measurements. Their commitment to producing a wide variety of high-quality samples in custom configurations is much appreciated.

Many thanks to the Night Vision & Electro-Optical Sensors Directorate (NVESD), Ft. Belvoir, VA for the gracious use of their indoor test facility and video recording equipment.

Without the fabrication and design efforts of Sam Barone, George Jaksha, and Kerry Yarber of NPS, my experimental measurements would have been much more difficult, and would have required at least three additional hands.

Professor Peter Crooker contributed greatly to this thesis, both in his capacity as Second Reader and as an experienced physicist. His explanations often made short work of the most puzzling challenges.

The successful completion of this thesis would not have been possible without my thesis Advisor, Professor Nancy Haegel. Her ability to pass along vast amounts of her



experience, knowledge, and wisdom, while simultaneously treating me both as a colleague and as an equal, made her a joy to work for, and contributed greatly to both my academic and professional development.

My greatest thanks go to my wonderful wife Riqui. Her unwavering devotion and encouragement during the past two years have made all of my other accomplishments possible.

## I. INTRODUCTION

### A. BACKGROUND

Fratricide is the unintentional injury or death of friendly personnel, or damage to friendly equipment, resulting from the use of weapons or munitions with the intent to kill the enemy or damage his equipment. Fratricide has always been a consequence of warfare, and the mitigation of this threat is an ongoing challenge to the modern warfighter, requiring much effort and planning.

Modern warfare often involves a large number of friendly forces, acting across a geographically wide battlefield. Operations may be conducted around the clock, in poor weather and in areas of poor visibility. Intelligence regarding the location of enemy (or even friendly) forces may be incorrect or incomplete.

Avoiding fratricide during ground engagements between individual "shooters" and their targets, is particularly challenging. Such engagements are often executed while friendly forces are on the move, with limited windows of time in which to engage targets of opportunity. Due to advances in modern weaponry, engagements often take place at great distances. In fact, the lethal range of an operator's weapons may far exceed the range at which he has satisfactory knowledge of the battle space and its inhabitants. Operational tempo, and resulting fatigue, also affect an operator's ability to accurately assess his surroundings, and identify friendly and enemy forces.

This lack of awareness, and the inability to positively identify friendly and enemy forces, are major contributing factors to fratricide. While advances in technology can enhance an operator's situational awareness and assist him in positive target identification, it is by no means a panacea. Technology has also increased the chance for potentially fatal error. Munitions fly farther and faster, and improved communications often mean that missions are assigned or changed with little notice, increasing the potential for confusion on the battlefield. This enhanced ability to communicate has also increased the operator's responsibility to keep his superiors informed of current conditions and mission status, adding to the operator's already heavy workload.

## **B. FRATRICIDE MITIGATION TECHNOLOGIES**

### **1. Glint Tape/GloTape®**

One technique that has been developed in order to reduce the possibility of fratricide is the use of "glint tape" or GloTape®. These are small wearable patches of material, designed to reflect incident infrared illumination back in the direction of the illumination source (Figure 1).



Figure 1. Infrared retro-reflective patches with U.S. markings (Night Vision Systems)

IR retro-reflective patches/tape are primarily intended for use in conjunction with the infrared illuminator/laser pointer devices attached to the rifles carried by friendly ground forces. When a friendly shooter unintentionally illuminates an individual wearing glint tape, the reflected infrared illumination is visible to the shooter through his night vision device, alerting him that he may have inadvertently targeted friendly forces, and prompting him to reevaluate the situation prior to engaging his target.

## 2. Infrared Beacons

Infrared beacons (Figure 2) are used to identify friendly personnel, mark buildings and structures, and assist in the location of isolated personnel during search-and-rescue (SAR) missions. Unlike IR reflectors, beacons do not require incident IR illumination, as they have their own battery-powered IR light-emitting diodes.



Figure 2. Wearable infrared beacon (Powerflare, Inc.)

The major disadvantage to IR beacons is that they are indiscriminate, emitting IR light whenever they are turned on, rather than requiring incident IR light in order to provide an emission via reflection. If the beacon is used

to identify friendly personnel, the wearer is essentially "advertising" his position to any observer with a near-infrared night vision device.

### 3. Individual Identification Friend or Foe (IIFF)

Another measure that has been developed recently is the Individual Identification Friend or Foe (IIFF) device. Designed at the Naval Postgraduate School, the IIFF device (Figure 3) is a small, flexible "patch" designed to be worn by friendly ground forces during nighttime operations.



Figure 3. Individual Identification Friend or Foe (IIFF) patch

A sensor in the patch responds to the illumination from the infrared laser pointer/illuminator mounted on the weapons of friendly ground forces. When a friendly

"shooter" unintentionally illuminates a friendly soldier wearing an IIFF patch, the sensor is activated and the patch responds by flashing in the near infrared (NIR) wavelengths. This response is visible to forces wearing NIR night vision devices (NVDs). The flashing response from the IIFF patch alerts the shooter that he may have inadvertently targeted friendly forces.

The NIR response is generated within the IIFF patch by using a visible-light flexible polymer light-emitting diode (PLED) [1] in conjunction with a flexible NIR long-pass filter. Although the primary emission from the PLED is in the visible part of the spectrum, the emission has a "tail" that extends into the NIR wavelengths with sufficient intensity to be easily observed through NVDs at ranges up to ~400 m.

The IIFF patch represents several improvements over the currently-fielded glint/GloTape® and IR beacons. While glint tape reflects all incident NIR illumination and beacons emit constantly, the IIFF patch is more covert because it only responds to illumination from friendly laser designators/target illuminators.

Because the flashing response from the IIFF patch continues for a fixed period of time after the patch is no longer illuminated, its response is more easily recognized compared to the response from glint tape, which may be difficult to discern against the background of incident light that the tape is reflecting.

### C. NIGHT VISION DEVICE PROLIFERATION AND SWIR

Current-generation NVDs are widely proliferated and available to both military and civilian users. As such, the NIR response from reflective tape, beacons and the current version of the IIFF patch may be visible to non-friendly (enemy or neutral) personnel equipped with NVDs.

The decision to extend the current IIFF design, to provide a response in the SWIR wavelengths, was driven by the desire to enhance the covert nature of the IIFF patch, and to make its response invisible to currently-fielded NVDs.

To this end, it was decided that the emission from the prototype SWIR version of the patch should begin at 1  $\mu\text{m}$  (1,000 nm) and extend to longer wavelengths. Current-generation NVDs are based on photoemission from GaAs cathodes. Therefore, their responsivity cuts off at  $\sim 900$  nm (Figure 4), so using SWIR wavelengths longer than 1  $\mu\text{m}$  will satisfy the requirement that the SWIR version of the IIFF patch be invisible to current-generation NVDs.



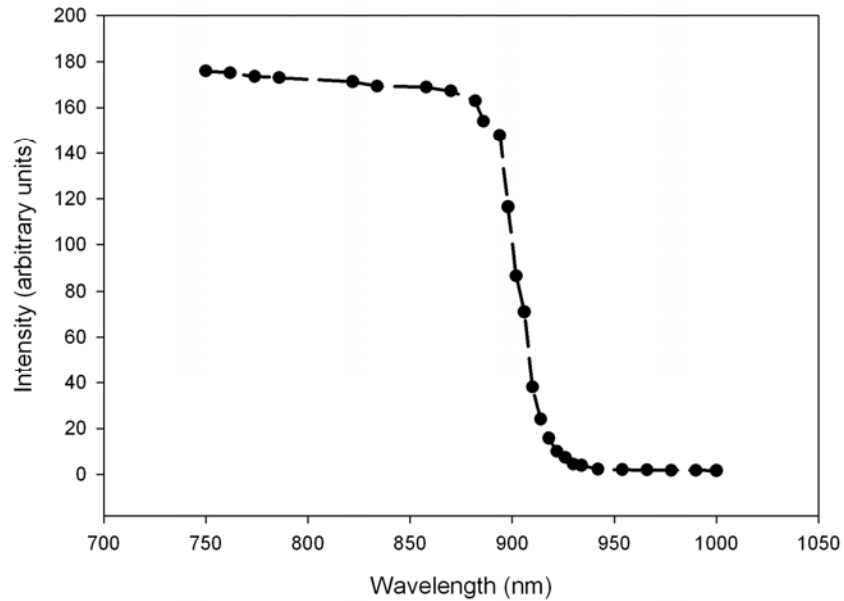


Figure 4. Responsivity of current-generation NVDs as a function of incident wavelength [From 2]

The behavior of SWIR radiation differs significantly from the behavior of the NIR emissions detected by current NVDs or those of the medium-wave (MWIR) emissions detected by thermal imagers (usually 3-5  $\mu\text{m}$  or 8-12  $\mu\text{m}$ .) SWIR is broadly defined as emission in the range from 1-2.5  $\mu\text{m}$ . Unlike MWIR, SWIR emissions are visible through glass. In addition, water vapor has a strong absorption at 1.4  $\mu\text{m}$  that makes foliage appear very bright. As a result, current foliage-patterned camouflage designs are ineffective in the SWIR region, providing additional advantages to SWIR-equipped forces. The use of SWIR-capable optics also allows observation of Nd:YAG 1.06  $\mu\text{m}$  and 1.54  $\mu\text{m}$  targeting lasers. Therefore, there is a growing interest in adding SWIR detectors to the multi-spectral capability provided to U.S. forces.

## II. DOWNCONVERTING PHOSPHOR FILTERS

### A. BACKGROUND/CONSIDERATIONS

In demonstrating a version of the IIFF patch that would produce its response in the SWIR region, it was desired to maintain the light weight, slim form factor, low power consumption and flexibility/durability of the NIR version of the IIFF patch. The emission mechanism of the NIR patch (a predominantly visible PLED in conjunction with a long-pass filter) was found to be unsuitable for producing a SWIR response. The spectral response of two PLED emitters is shown in Figure 5. None of the commercially-available visible-light PLEDs produced a response that extended far enough into the SWIR wavelengths to be used directly as a SWIR source.

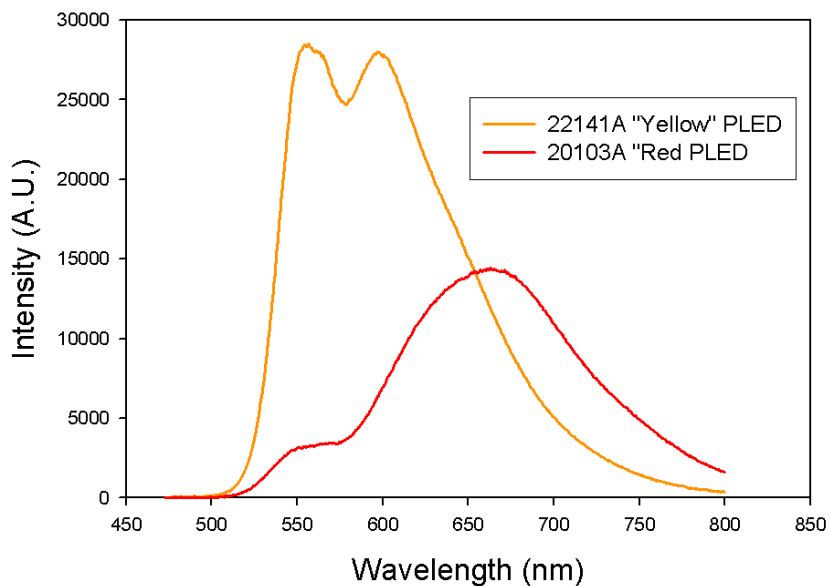


Figure 5. Visible Spectra of red and yellow PLED visible emitters

To achieve acceptable output intensity in the SWIR region, a two-step mechanism was devised, whereby a visible-wavelength PLED was used to illuminate a phosphor filter. The phosphor filter absorbs the visible photons and emits lower-energy photons in the SWIR wavelengths. This process is known as "downconversion", and is utilized in a variety of areas, including non-linear optics, solid state lighting and increasing the efficiency of solar cells.

Quantitatively evaluating the various combinations of visible-light emitters and downconverting phosphors requires three distinct measurements: 1) Using photoluminescence excitation spectroscopy (PLE) to measure the phosphor's optical response to various wavelengths of incident visible light, 2) SWIR spectroscopy, to measure the SWIR emission of the excited phosphor, and 3) Visible-light spectroscopy to measure the spectra of the various PLED devices, in order to determine which PLED would most efficiently excite the phosphor filters, and produce a SWIR output.

#### **B. PHOTOLUMINESCENCE EXCITATION SPECTROSCOPY**

To evaluate the various phosphor filter samples, photoluminescence excitation spectroscopy (PLE) measurements were performed. PLE is a technique in which the energy of the incident optical excitation is varied while measuring the intensity of the resulting luminescence. This technique is of value in correlating optical absorption directly to a given emission and for determining which visible wavelengths excite the phosphor filters most efficiently.

The phosphor samples were provided by Add-Vision, Inc. of Scotts Valley, California. The samples were produced by mixing a phosphor pigment into a paste, which was then screen-printed onto a plastic substrate. The thickness of the phosphor pigment layer was determined by the number of "passes" made during the screen-printing process. The primary advantage of this method of depositing the phosphor is that the printing process does not require sophisticated equipment, and the process need not be performed under a vacuum or in a sterile environment.

The various samples differed in the phosphor pigment used, the substrate upon which the pigment was deposited, the thickness of the pigment layer, and whether they were excited with visible light incident on the pigment side of the sample or the substrate side of the sample. The following naming convention was used to designate samples:

S-SWIRXX-TI

where 'S' denotes the type of substrate used, 'XX' denotes which type of pigment was used, 'T' represents the thickness of the pigment layer, and 'I' represents the direction of the incident light.

The possible values for 'S' are:

- A - Clear Polycarbonate, 120  $\mu\text{m}$
- B - Clear Polycarbonate, 160  $\mu\text{m}$
- C - Matte Polycarbonate, 120  $\mu\text{m}$
- D - Matte Polycarbonate, 160  $\mu\text{m}$
- E - Polyethylene Terephthalate, 90  $\mu\text{m}$
- F - Polyethylene Napththlate, 100  $\mu\text{m}$

The values for XX are:

06 - Nd<sup>3+</sup> - based phosphor

07 - Yb<sup>3+</sup> - based phosphor

09 - Nd<sup>3+</sup> - based phosphor with Rhodamine dye added

The values for 'T' represent the number of layers of phosphor pigment printed on the substrate, with more layers resulting in a thicker pigment layer. Sample thicknesses ranged from 18 μm to 45 μm.

The visible excitation light is incident upon:

S - Substrate side of the sample

P - Pigment side of the sample

As an example, the designation "A-SWIR06-4S" denotes a sample of the SWIR06 phosphor deposited four layers thick on a 120 μm clear polycarbonate substrate and illuminated from the substrate side of the sample.

The PLE measurements were performed using a 100 W / 6.3 A tungsten lamp as the visible light source. A schematic of the full system is shown in Figure 6.

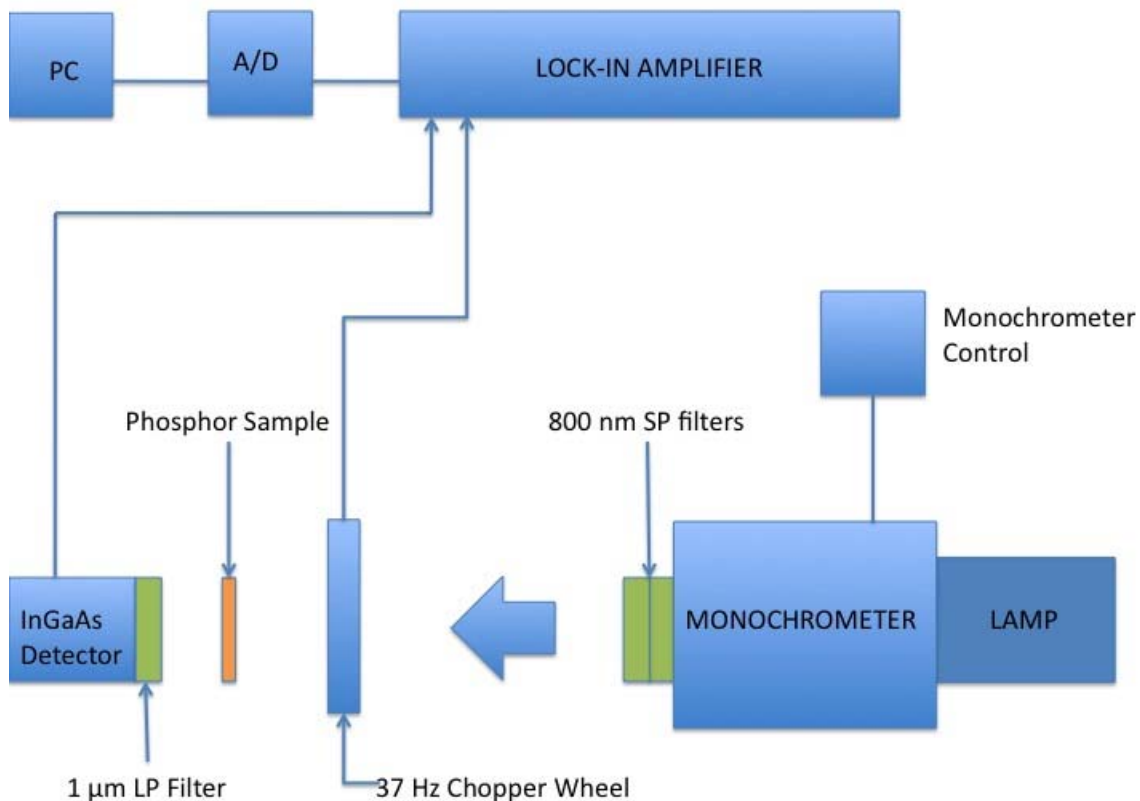


Figure 6. PLE Experimental setup

The light from the tungsten lamp was passed through a quarter-meter Photon Technologies International monochromator in order to isolate a single visible wavelength. While this monochromator has a stray light rejection of approximately  $10^{-4}$ , in the presence of a very bright source and/or a low measured emission from the phosphor, this can result in observation of stray SWIR emission from the excitation source that is comparable in intensity to the SWIR emission from the downconverting phosphor sample. In order to block the stray SWIR emission from the tungsten lamp, the output from the monochromator was passed through two stacked 800 nm short-pass edge filters purchased from Newport Corporation [3].

The filtered light from the monochrometer was then used to illuminate the phosphor sample. A cooled Hamamatsu G6122 SWIR photodetector was placed on the opposite side of the phosphor sample to detect the resulting SWIR emission from the downconversion taking place in the phosphor. To ensure that the detector only responded to the desired wavelengths, a 1  $\mu\text{m}$  Newport long-pass edge filter was placed over the detector input to block out shorter-wavelength NIR illumination as well as any visible incident light that was transmitted through the phosphor sample without being absorbed.

To more easily separate the photodetector's response from its background noise, a chopper wheel was placed immediately prior to the phosphor sample, and connected to a Princeton Applied Research Model 5210 lock-in amplifier. The chopper wheel imparted a modulation frequency of 37 Hz to the illumination incident on the phosphor, allowing the lock-in amplifier to better isolate the resulting signal from the photodetector's near-DC background noise. The output voltage of the lock-in amplifier is proportional to the total SWIR output of the sample from 1  $\mu\text{m}$  out to a maximum wavelength of 2.05  $\mu\text{m}$  (the long-wavelength limit of the photodetector.)

The output voltage of the lock-in amplifier was recorded with a Keithley KUSB-3108 A/D converter connected to a Dell laptop running the "Quick Data Acquisition" software package from DTx-EZ. The "Strip Chart" function of the software was used to record the amplifier voltage as the monochrometer output was swept linearly from 400 nm to 800 nm over a period of approximately 90 seconds.

For these samples, the settings used on the lock-in amplifier were:

Sensitivity: 100 mV or 300 mV, based on emitter intensity

Integration Time Constant: 100 ms

Filter: Flat (none)

After all of the PLE curves for a particular phosphor type were recorded, they could be compared to one another using the magnitude of the peak response, since all of the curves from similar phosphors had the same shape. To compare the integrated SWIR output of one sample against a sample of another type of phosphor, the total areas under the excitation curves from 400-800 nm were calculated and compared.

## **1. SWIR06**

The SWIR06 pigment is based on a rare-earth phosphor (neodymium 3+). The energy level diagram of Nd<sup>3+</sup> is shown in Figure 7. Neodymium is commonly used for its emission at 1.06  $\mu\text{m}$  in applications such as the Nd:YAG (neodymium/yttrium/aluminum/garnet) laser.



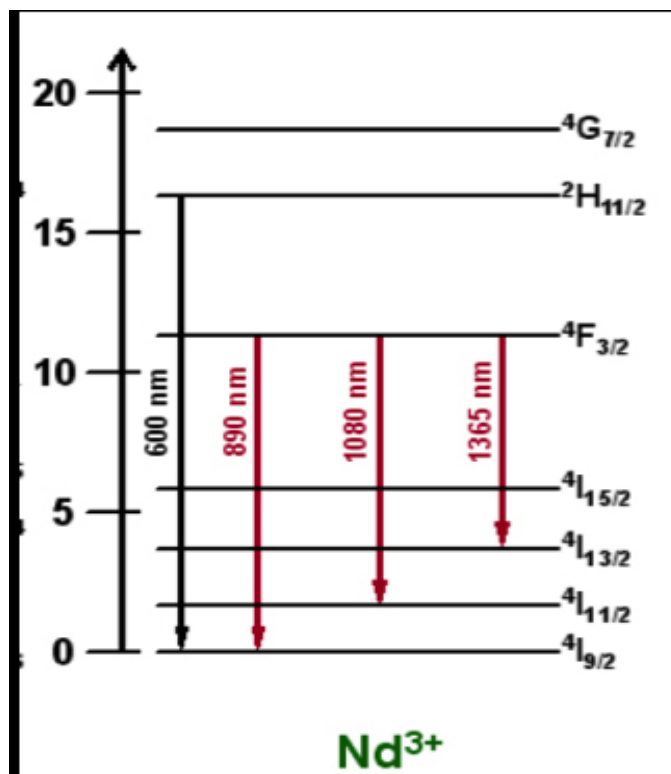


Figure 7. Energy level diagram for Nd<sup>3+</sup> (energies in 10<sup>4</sup> cm<sup>-1</sup>) [From 4]

Eight initial SWIR06 samples were produced, with various pigment thicknesses placed on several different substrates. The PLE Spectra that follow show that all of the samples, regardless of configuration, were best excited by incident visible light with a wavelength of approximately 640 nm. The width of the excitation peak extended from approximately 550 nm to 720 nm. There were also smaller secondary excitation peaks at approximately 480 nm and 750 nm.

To judge the effects of varying the sample parameters (substrate type, pigment thickness, and incident light direction), comparisons were performed on multiple samples that only differed in one parameter. Figure 8 shows the PLE

spectra of several samples on different substrates. The choice of substrate was found to have a measurable (although minor) effect on SWIR output - up to approximately five percent.

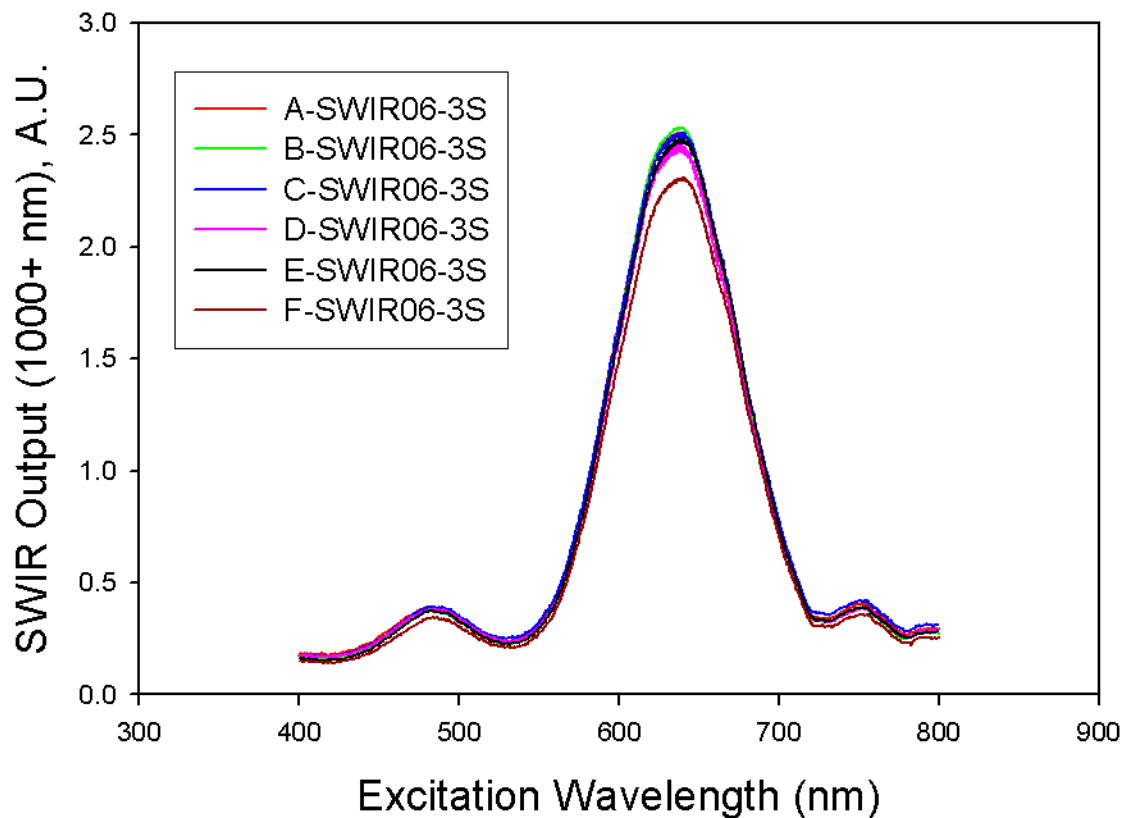


Figure 8. PLE spectra (output as a function of excitation wavelength) showing effect of different substrate materials on SWIR output

Likewise, the direction of incident visible illumination did not have a great effect on SWIR output from the sample. Figure 9 shows the response of a phosphor sample illuminated from both the substrate side and the pigment side. Even among samples utilizing the same

substrate, there was no clear trend showing illumination from the substrate side or the pigment side to be superior even by a small amount, with the differences in SWIR output intensity being generally less than 10%.

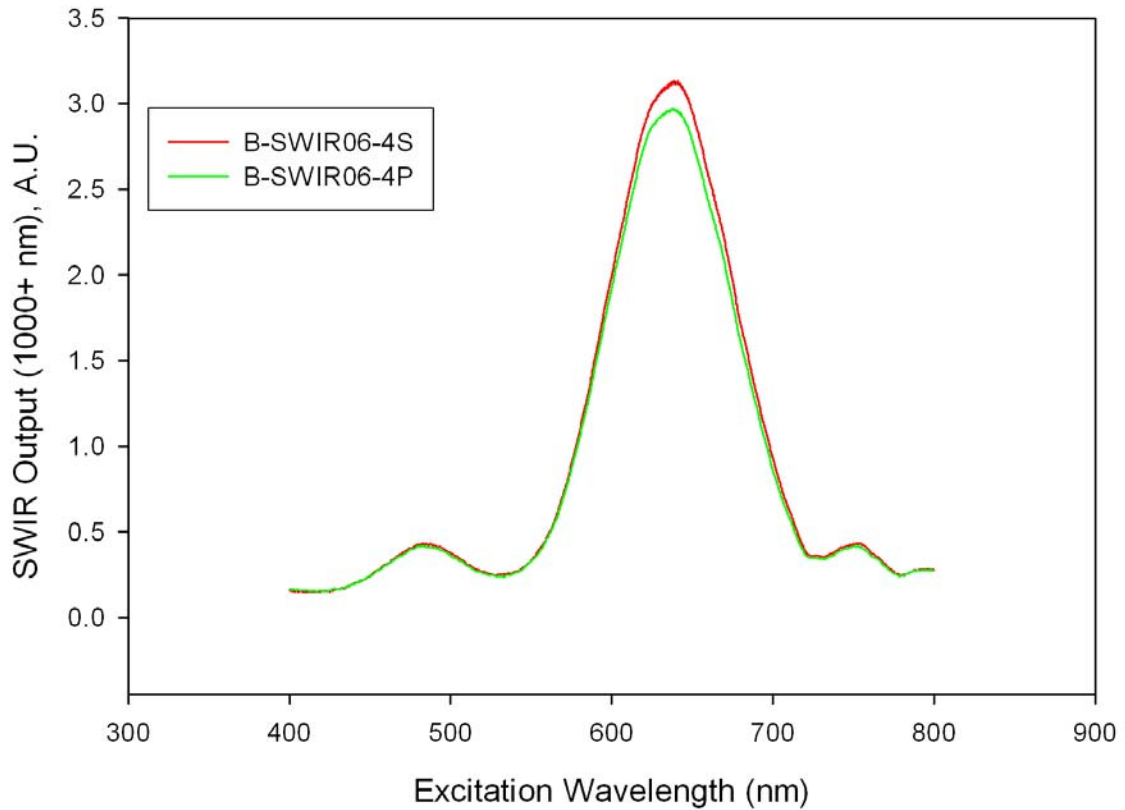


Figure 9. PLE spectra showing effect of illumination direction on SWIR output

The thickness of the pigment had the greatest effect on the SWIR output. Among the SWIR06 samples, the thicker pigment layers consistently produced higher SWIR measurements when compared to the thinner pigment layers. Figure 10 shows the response of SWIR06 samples of varying pigment thicknesses from 20  $\mu\text{m}$  to 30  $\mu\text{m}$ .

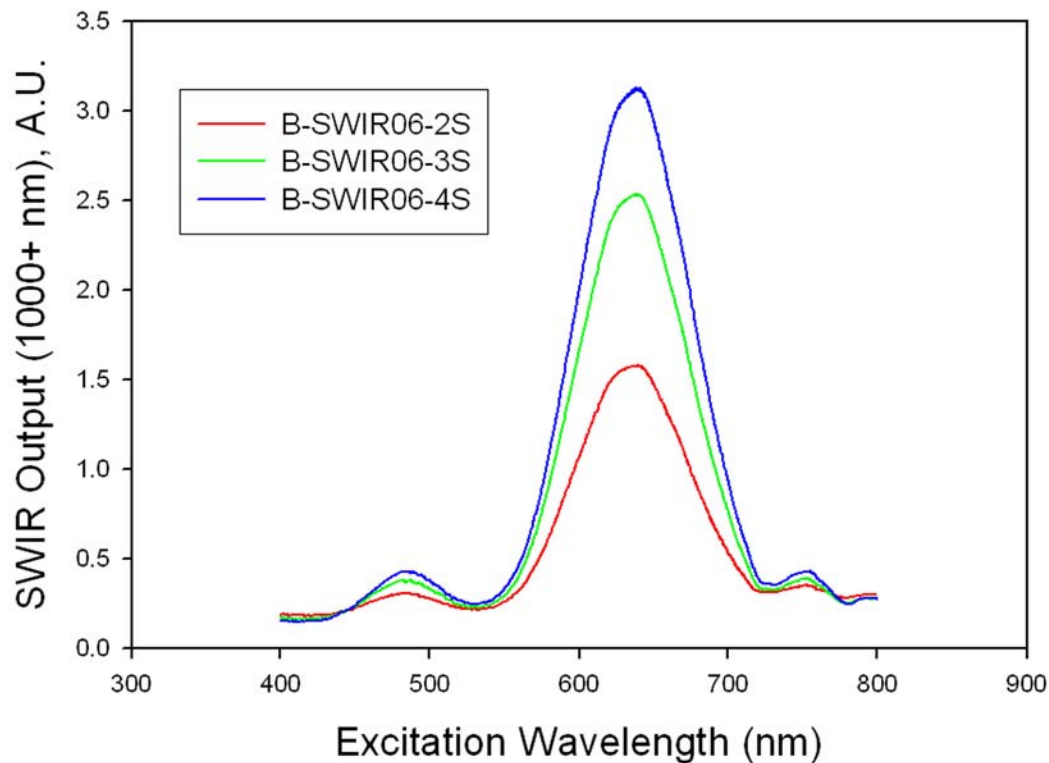


Figure 10. PLE spectra showing effect of pigment layer thickness on SWIR output. Estimated thicknesses are: red - 20  $\mu\text{m}$ , green - 25  $\mu\text{m}$ , blue - 30  $\mu\text{m}$ .

Based on the results from the first batch of eight samples, additional samples were produced in order to explore particular combinations of optimized parameters that were not present in the first batch. Because of changes in the PLE measurement setup, the voltages in the following figures cannot be directly compared to the voltage values from the first batch. The best sample from the first batch (B-SWIR06-4S) was re-tested using the new experimental configuration, and its results included in the following figures, so that the second-round samples can be quantitatively compared to the previous samples.

The second batch of samples included several with thicker pigment layers than those from the first batch. Consistent with the earlier results, total SWIR output continued to increase as the thickness of the pigment layer was increased, out to the maximum measured thickness of 45  $\mu\text{m}$ . This indicates that further gains may be realized by using even thicker pigment layers in the future. Figure 11 shows the response of several of the newer samples compared with the best sample from the first batch (B-SWIR06-4S).

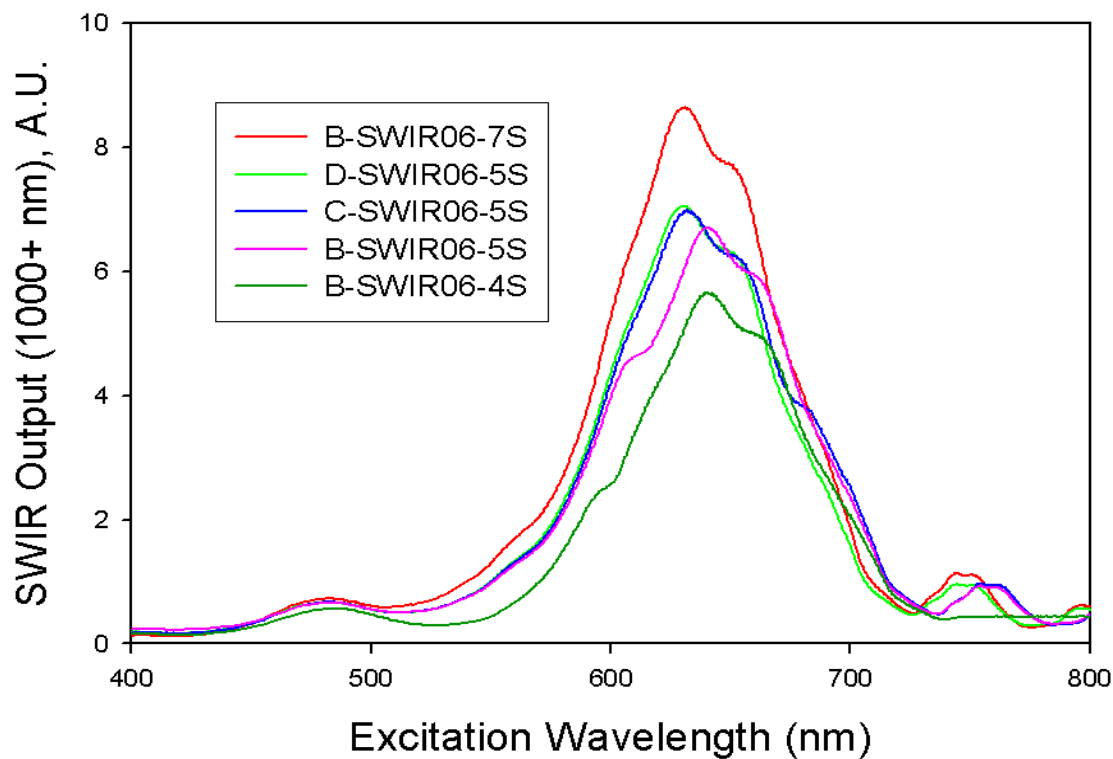


Figure 11. PLE showing improved response from thicker pigment layers compared to best sample from first batch (B-SWIR06-4S)

The appearance of additional structure in the PLE curves shown in Figure 11 are believed to be the result of mechanical friction in the monochromator causing a variation in the scan rate during the sweep from 400 nm to 800 nm. In the future, it may be beneficial to reproduce the experimental data by performing a higher-resolution PLE measurement.

## 2. SWIR07

The SWIR07 pigment is believed to be based on Ytterbium  $3^+$ . The energy level diagram is shown in Figure 12. The SWIR07 Pigment showed strong absorption at two different excitation wavelengths, 592 nm and 760 nm. There were also two smaller absorption peaks near 525 nm and 690 nm. With similar pigment layer thicknesses, the peak excitation of the SWIR07 samples was higher than that of the SWIR06 samples, although the excitation peaks are not as broad. Figure 13 shows the PLE response curve of a typical SWIR07 sample.

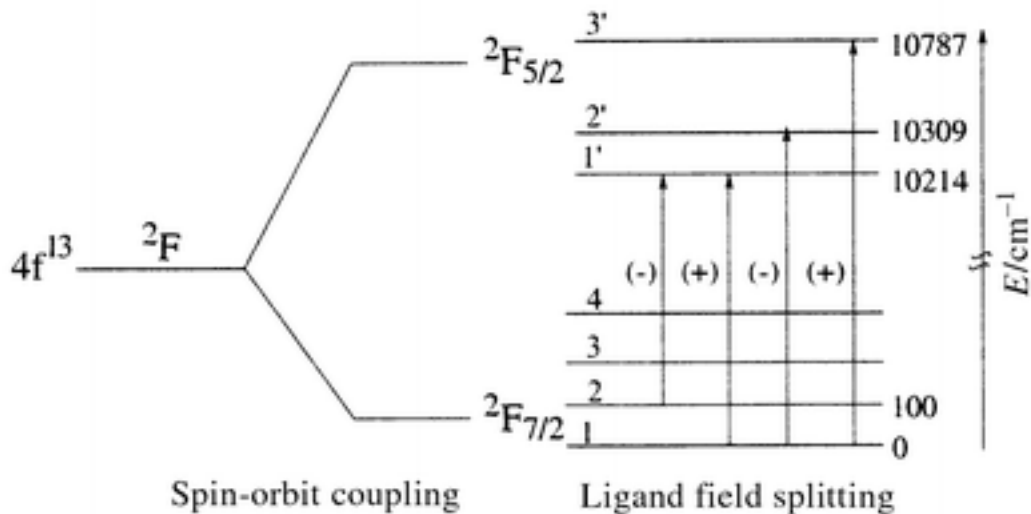


Figure 12. Energy level diagram for  $Yb^{3+}$  [From 5]

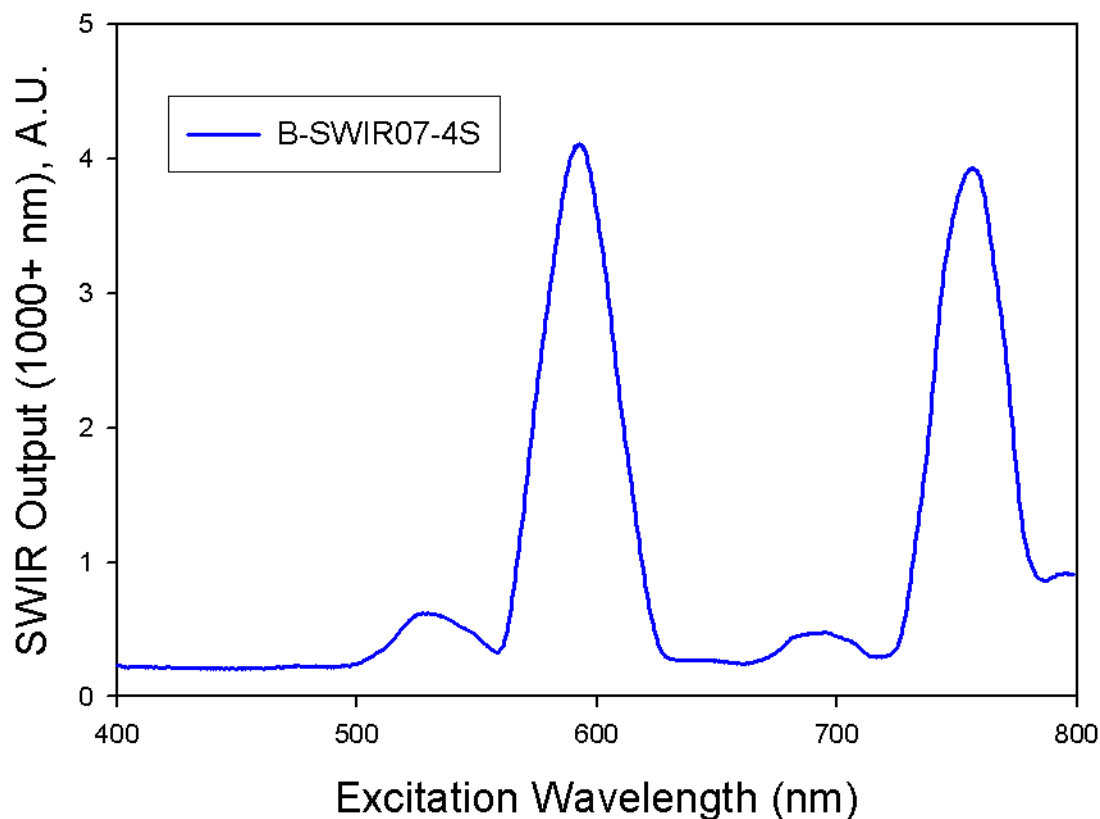


Figure 13. PLE response curve of SWIR07  $\text{Yb}^{3+}$ -based phosphor pigment

The initial batch of samples contained three SWIR07 samples, all on the same substrate, but with differing pigment layer thicknesses. As was the case with the SWIR06 samples, varying the thickness of the pigment layer had a significant effect on the total SWIR output. Figure 14 shows the PLE response curves for the three SWIR07 samples in the initial batch.

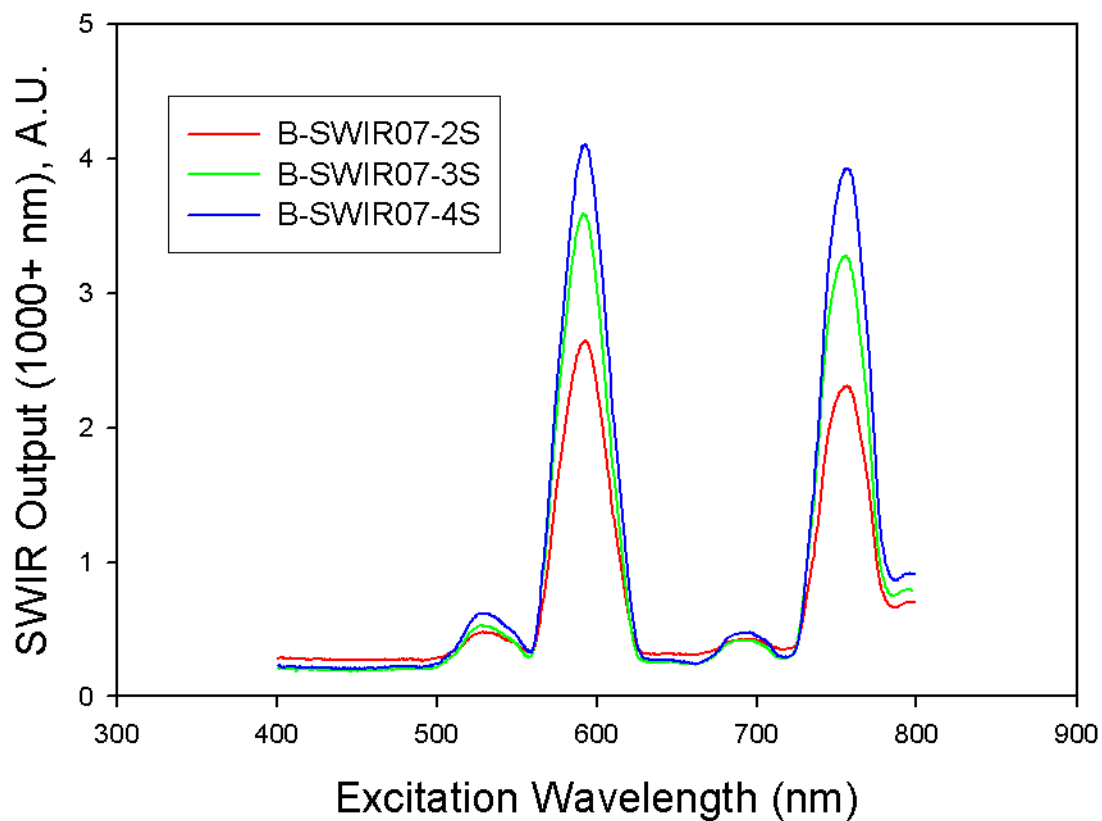


Figure 14. PLE spectra showing effect of pigment layer thickness on SWIR emission

Consistent with the results for SWIR06, the excitation of the SWIR07 phosphor did not depend strongly on the direction of incident illumination. Figure 15 shows the responses from one SWIR07 sample illuminated from the substrate side and from the pigment side.



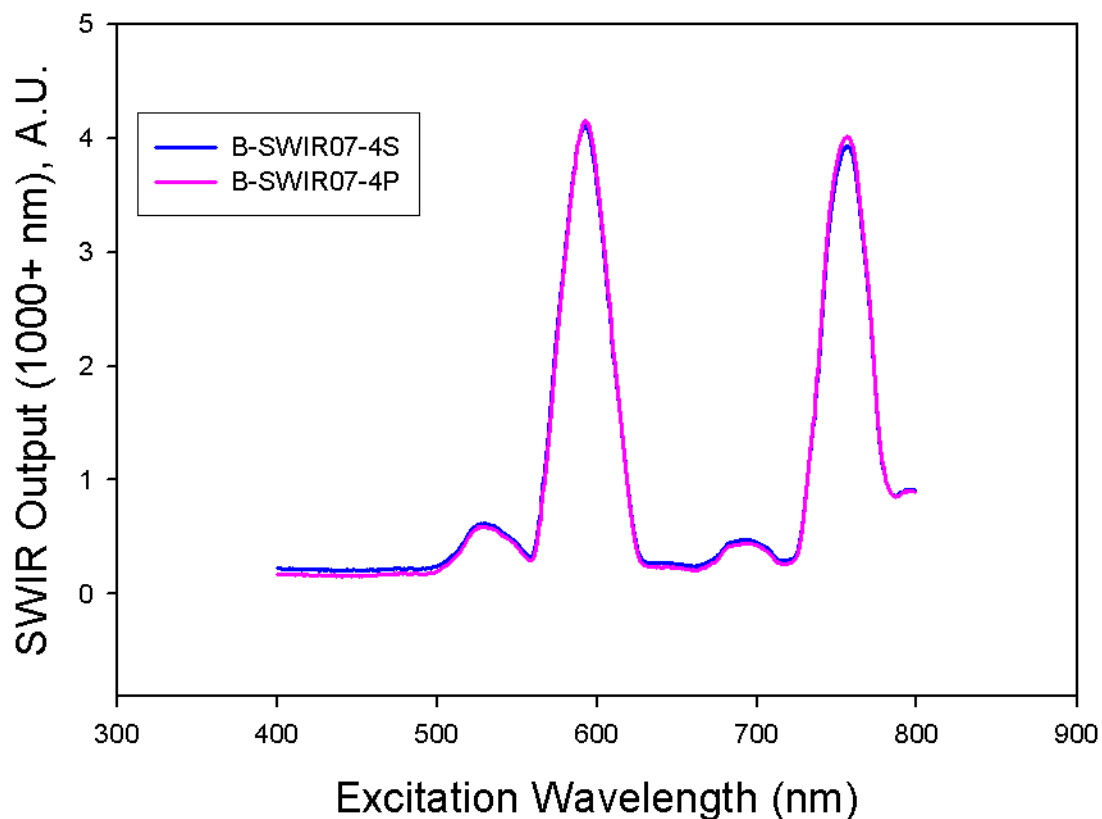


Figure 15. PLE spectra showing effect of direction of incident illumination on SWIR emission

Five additional SWIR07 samples were produced using different substrates and thicker pigment layers. The increase in pigment layer produced an increase in total SWIR output, up to the maximum available thickness of 38  $\mu\text{m}$  (Figure 16.) As with the SWIR06 samples, the magnitudes in Figure 6 cannot be compared directly to the measurements from the initial batch, but the best sample from the initial batch (B-SWIR07-4P) was retested with the new equipment configuration and included in the figure. Although it did not affect the final conclusions, friction in the monochromator drive gear caused a horizontal shift in

several of the response curves in Figures 16 and 17, as well as requiring the termination of the measurements prior to recording the second large excitation peak near 760 nm.

As was the case with the SWIR06 phosphor, it appears that the SWIR07 phosphor will benefit from further increases in pigment thickness.

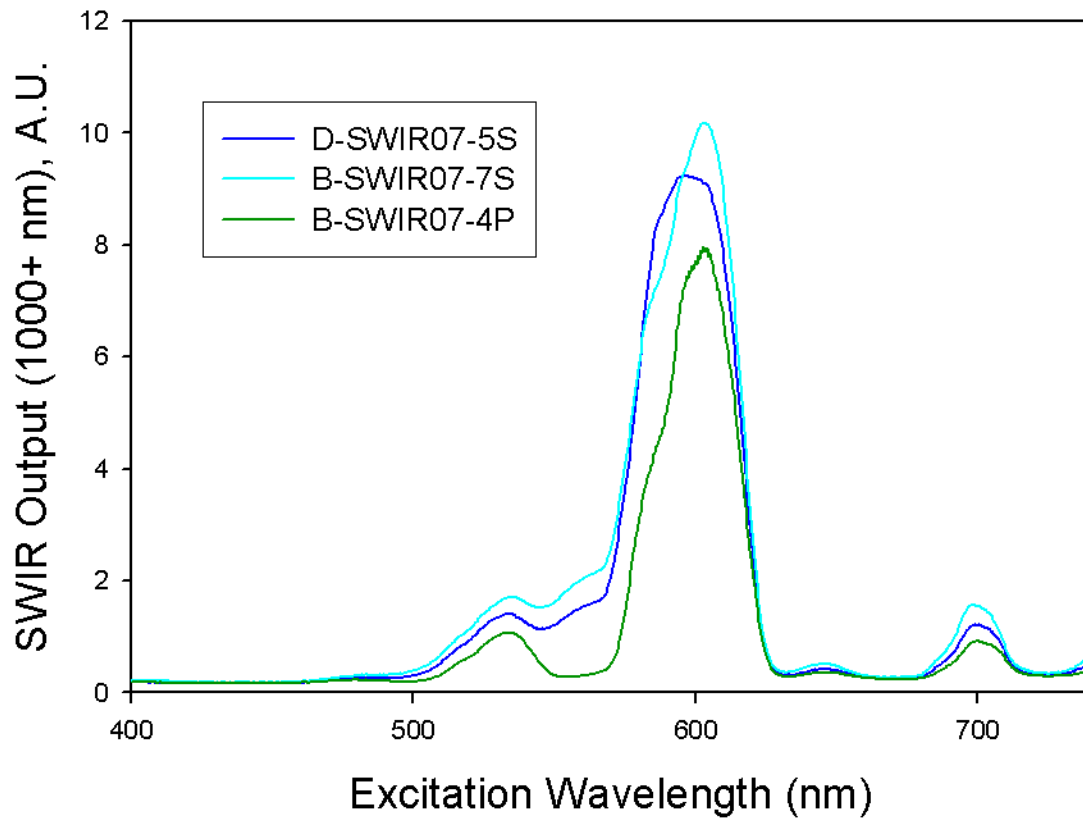


Figure 16. PLE spectra showing improved response from thicker pigment layers compared to best sample from first batch (B-SWIR07-4P)

The choice of substrate did not have a large effect on the total SWIR emission from the SWIR07 phosphor. Figure 17 shows the PLE curves for three samples of equal thickness on different substrates.

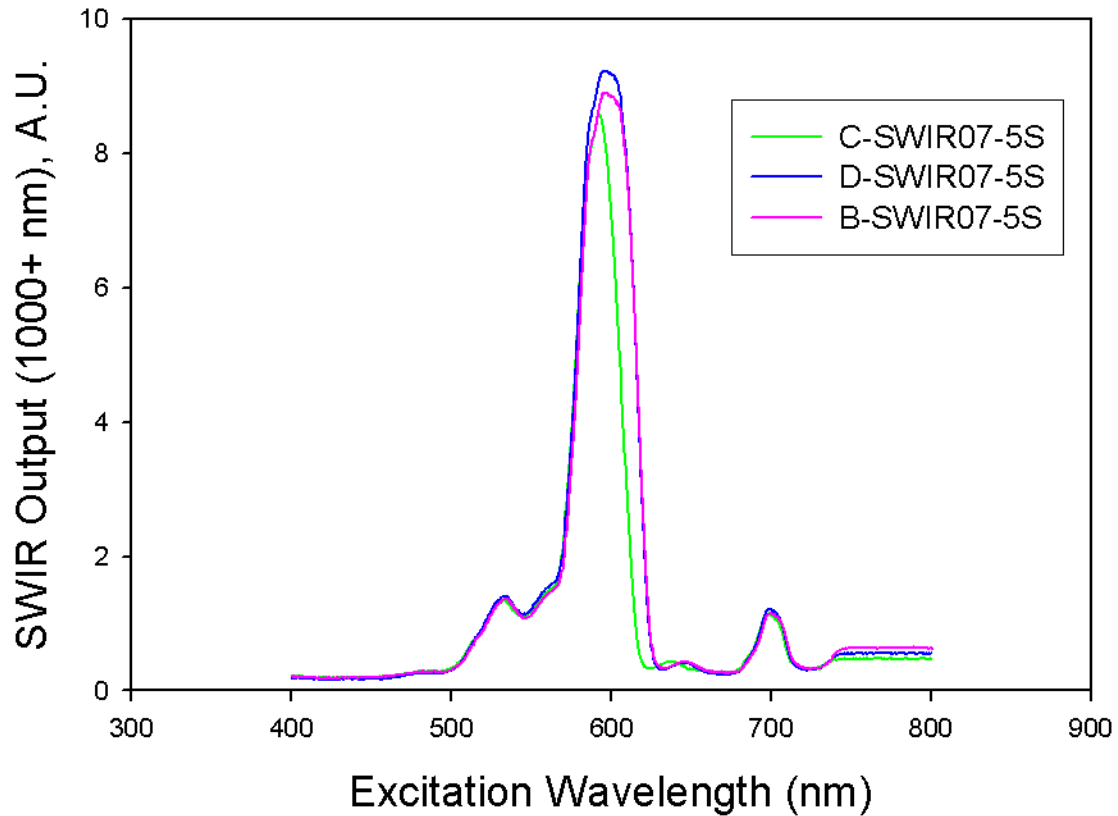


Figure 17. PLE spectra showing effect of various substrates on SWIR emission

### 3. SWIR09

The SWIR09 samples use a pigment that is a mixture of the same  $\text{Nd}^{3+}$  phosphor used in the SWIR06 samples and a fluorescent Rhodamine dye. The Rhodamine dye is designed to absorb visible photons near 543 nm and emit photons at 625 nm, which would then excite the  $\text{Nd}^{3+}$  phosphor in the

phosphor pigment into producing a SWIR emission. Since the  $\text{Nd}^{3+}$  phosphor shows very little absorption near 543 nm, the photons used to excite the Rhodamine dye are not being "cannibalized" from the photons used to directly excite the phosphor. By converting these otherwise-unused visible photons into photons that would more efficiently excite the phosphor, it was hoped to increase the total SWIR output compared to a pigment utilizing only the  $\text{Nd}^{3+}$  phosphor.

Figure 18 shows the PLE results of three SWIR09 samples along with the response of a SWIR06 sample for comparison. As in the SWIR06 samples, the peak total SWIR emission corresponded with an excitation wavelength of approximately 640 nm.

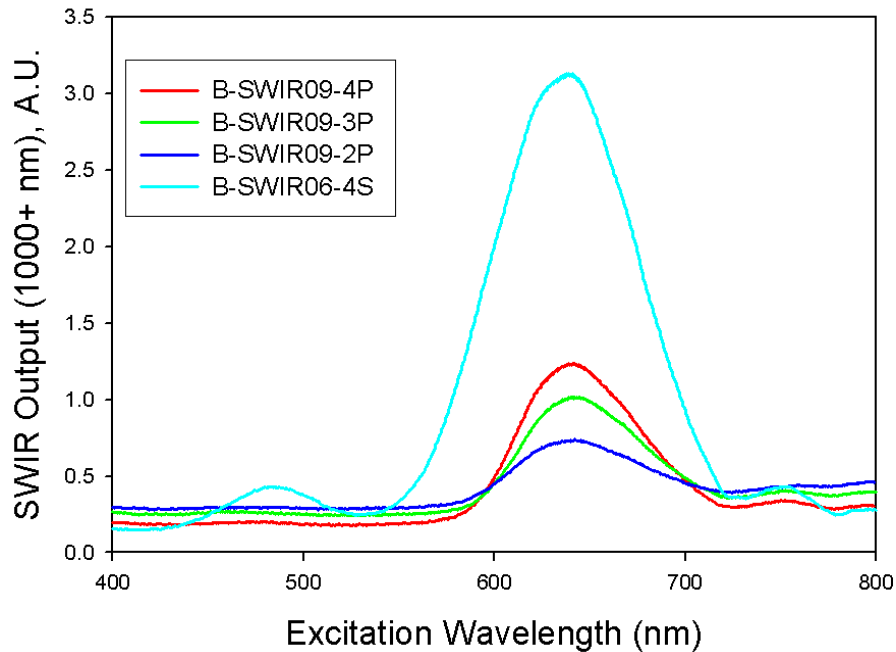


Figure 18. PLE results for three SWIR09 samples, with best SWIR06 sample (B-SWIR06-4S) shown for comparison

The PLE results for the SWIR09 samples showed a marked reduction in total SWIR output compared to a SWIR06 sample of equivalent thickness. Not only is the total SWIR response of the B-SWIR09-4P sample approximately 60% lower than that of the SWIR06 sample of similar thickness, the PLE curve shows virtually no SWIR output at an excitation wavelength of 543 nm where the visible-to-visible conversion from the Rhodamine dye should have occurred. This could be a result of poor conversion efficiency in the Rhodamine dye, or it could be that the longer-wavelength photons produced by the Rhodamine dye were not being absorbed by the phosphor pigment. The introduction of the Rhodamine dye into the phosphor pigment also meant that there was a lower phosphor concentration compared to a phosphor-only sample of equal thickness. No further SWIR09 samples were investigated, pending further research into the optimum ratio of Rhodamine dye to phosphor pigment.

### **C. SWIR EMISSION SPECTRA**

The PLE measurements were used to determine which incident visible wavelengths most efficiently excited the phosphor samples, as well as to determine which phosphor sample produced the greatest peak SWIR output at wavelengths greater than 1  $\mu\text{m}$ .

It was also necessary to determine which particular wavelengths of SWIR output were produced by the various phosphors when they were excited with the optimum wavelength of incident visible light. To perform this measurement, the phosphor sample was excited by light from the monochromator at the optimum excitation wavelength(s) determined in

Chapter II(b). An Ocean Optics NIR-512 spectrometer was used to measure the emitted IR light in the range from 854-1740 nm.

Since the desired SWIR output was in the range of 1  $\mu\text{m}$  and longer, the SWIR spectra allowed a determination of how much of the total SWIR output was “usable” for covert IIFF purposes. A strong emission below 1000 nm was not useful, because these wavelengths could be visible to current-generation NVDs and must be filtered out of the total SWIR emission from an actual device.

### 1. SWIR06

Figure 19 shows the SWIR spectrum of the SWIR06 phosphor when excited by incident light at 640 nm. The spectrum shows three double peaks in the phosphor’s SWIR output. The first two peaks are at approximately 880 nm and 940 nm, with the other two double peaks located at approximately 1080/1120 nm and 1330/1420 nm.

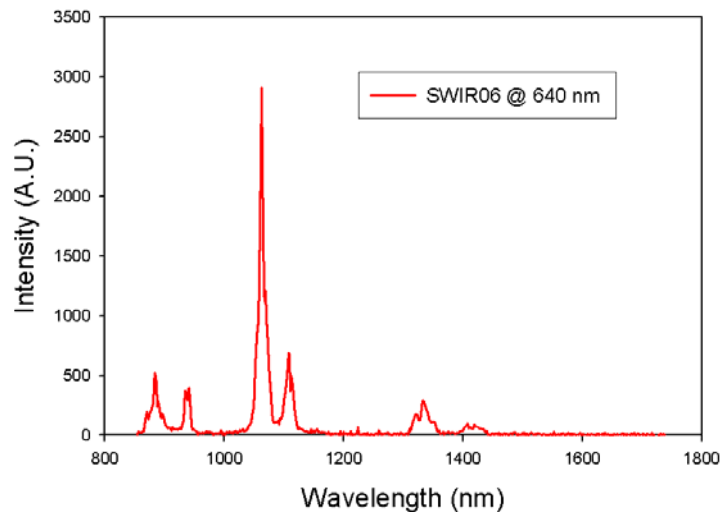


Figure 19. SWIR emission from SWIR06 phosphor excited by 640 nm light

The double peaks in the emission spectrum are likely due to local stresses and field effects within the phosphor/host mixture which break the degeneracy of the excited energy levels in the neodymium ions. Examples of these effects are Stark shifting and the Ligand field effect. These effects cause individual transitions in the energy level diagram to be replaced by multiple transitions of similar energies.

The emission peaks at 880 nm and 940 nm are below the usable threshold wavelength, but the wavelengths greater than 1  $\mu\text{m}$  account for approximately 80.3% of the total SWIR emission, as determined by summing the photon counts from the spectrometer from 1000 nm to 1740 nm and dividing this total by the sum over all measured wavelengths.

## **2. SWIR07**

Because the SWIR07 phosphor was excited by incident visible light at 592 nm, as well as 758 nm, two SWIR spectra were measured, one for each excitation wavelength (Figures 20 and 21.) The shapes of both spectra were virtually identical, differing only in amplitude.

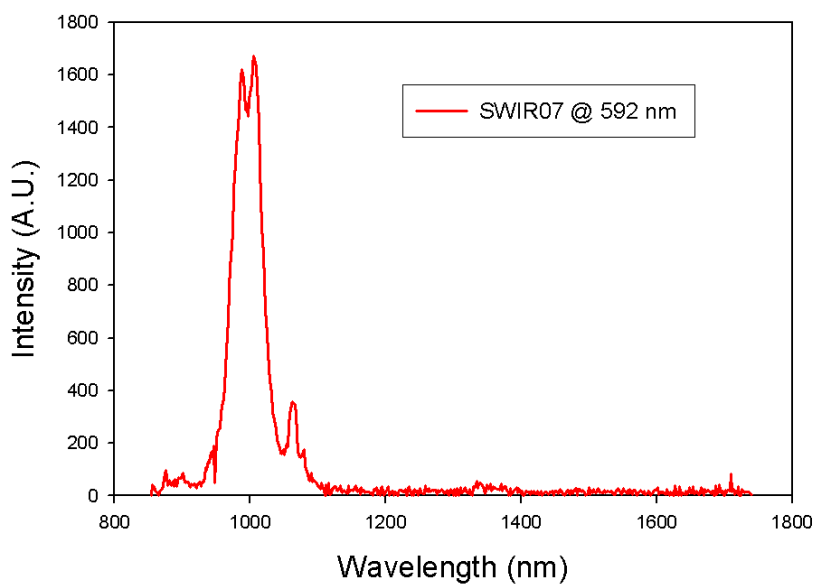


Figure 20. SWIR emission from SWIR07 phosphor excited by 592 nm light

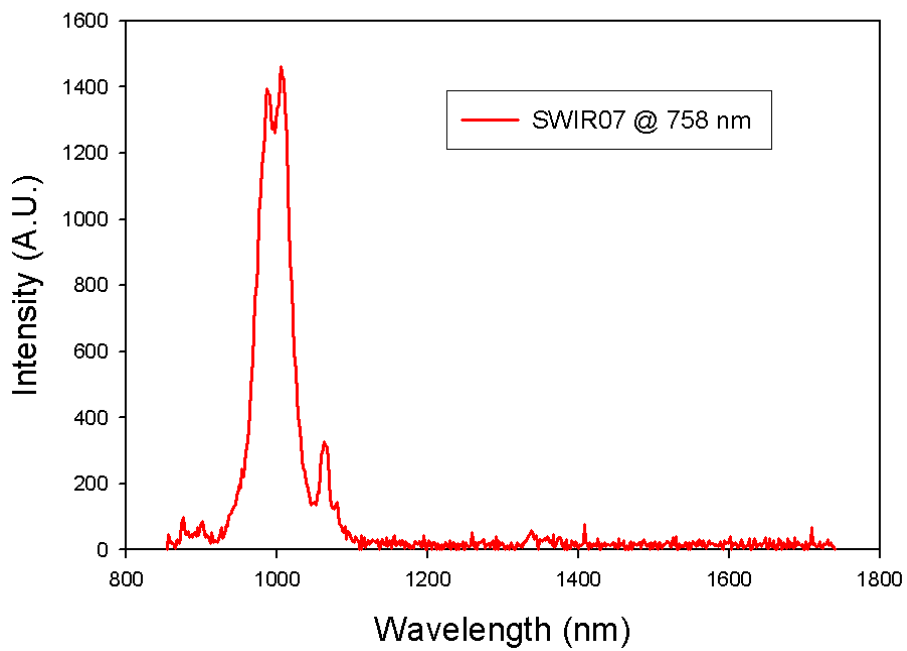


Figure 21. SWIR emission from SWIR07 phosphor excited by 758 nm light



The emission in the SWIR07 phosphor consisted primarily of a single peak centered at 1  $\mu\text{m}$ , with a much weaker emission at 1.05  $\mu\text{m}$ . Because of the location of peak's center wavelength, nearly half of the emitted SWIR light is at wavelengths shorter than 1  $\mu\text{m}$ . Only approximately 53% of the SWIR emission is at wavelengths beyond 1  $\mu\text{m}$ .

### 3. SWIR09

Similar to the SWIR06 phosphor, the SWIR09 phosphor was excited most efficiently by incident light at 640 nm. The SWIR emission spectrum is shown in Figure 22. The location of the emission peaks is the same as in the SWIR06 samples, but the peak amplitude is much lower, consistent with the PLE measurements. Approximately 82% of the total SWIR emissions occur at wavelengths greater than 1  $\mu\text{m}$ .

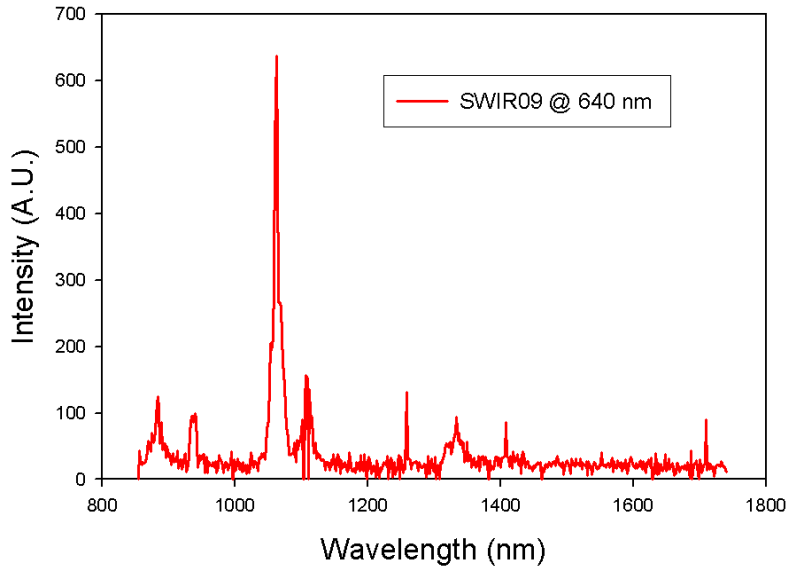


Figure 22. SWIR emission from SWIR09 phosphor excited by 640 nm light

### **III. POLYMER LIGHT-EMITTING DIODES**

The visible light source used to illuminate the phosphor downconverting filter will be a polymer light emitting diode (PLED), powered with a current of 3 mA per square centimeter of polymer at a voltage of approximately 15 V. For the NIR version of the IIFF patch, the NIR emission was obtained by filtering the visible light output from the PLED with a 750 nm long-pass filter. This meant that the ideal PLED emission for the NIR IIFF patch was engineered toward the longer visible wavelengths in order to maximize the NIR "tail" in the longer wavelengths of the PLED's emission spectrum.

For the SWIR IIFF patch, it was determined that the emission spectrum from the PLED did not extend far enough into the SWIR wavelengths for the PLED to be used directly as a SWIR source. This necessitated the two-step visible-to-SWIR downconversion process, and the pigment formulation in the PLED was selected so that the visible light emission would more closely match the required visible excitation wavelengths of the phosphor filters. Two options, a red and a yellow PLED material, were evaluated.

#### **A. RED EMITTER**

##### **1. Visible Light Spectra**

The visible spectra of the "red" PLED was measured using an Ocean Optics USB-4000 spectrometer. A 1 cm<sup>2</sup> sample of the PLED was powered with a 3 mA current from a Keithley 220 current source, with a compliance voltage of 36 V. The

PLED sample and fiber-optic input cable from the spectrometer were placed in a jig so that the end of the fiber-optic cable was fixed approximately two centimeters from the sample. The spectrometer was controlled using the Ocean Optics "Spectra Suite" software package, with the following settings:

High Gain Mode : On

Integration Time : 1 s

Boxcar Width : 0

Figure 23 shows the visible spectrum of the "red" PLED sample along with the spectrum of the "yellow" PLED sample described in the next section. Since the intensity of the PLED emission is known to be time-dependent [6], the samples were biased for a fixed period of 20 seconds prior to obtaining the spectra.

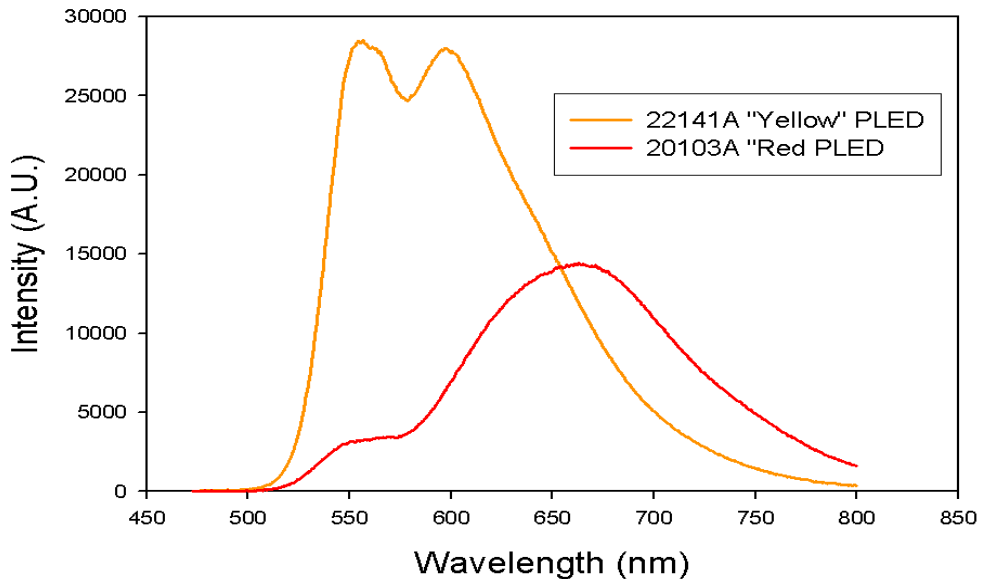


Figure 23. Visible emission spectra of "red" and "yellow" PLED spectra.

The peak light output from the red sample occurs at a wavelength of ~660 nm. This wavelength is too long to effectively excite the SWIR06 phosphor at its peak excitation wavelength of 640 nm. The red PLED was also suboptimal for use with the SWIR07 phosphor, which has excitation peaks at 592 nm and 758 nm. Since the SWIR09 samples use the same phosphor as the SWIR06 samples, the red PLED performed poorly with those samples as well. In addition, the Rhodamine dye used in the SWIR09 samples has a peak excitation of 543 nm, so the red PLED would not effectively excite the dye.

#### **B. YELLOW EMITTER**

The visible spectrum of the yellow PLED emitter was measured using the same equipment settings and software as the red sample. As shown in Figure 23, the peak output of the yellow PLED occurred at a shorter wavelength, with two peaks at approximately 540 nm and 600 nm. The output of the red PLED was slightly higher at 760 nm, but for all wavelengths shorter than 650 nm, the output of the yellow PLED was significantly greater than the red PLED, making it the better choice for exciting the SWIR phosphor samples.

THIS PAGE INTENTIONALLY LEFT BLANK

#### IV. COMBINED EFFECTIVENESS OF PLED/SWIR COMBINATION

The overall SWIR output of the emitter/phosphor combination was evaluated by using SigmaPlot to perform a point-by-point multiplication of the visible-light output spectrum from the PLED by the PLE curve of the phosphor sample. This convolution was necessary because a bright emission from the PLED at a particular wavelength will not produce very much SWIR output from the phosphor if the excitation of the phosphor is weak at that wavelength. Likewise, a strong absorption in the phosphor at a particular wavelength is not useful if that wavelength is not present in the PLED emission spectra.

Performing the multiplication required tailoring of the data sets, because the visible light spectra consisted of 3500 measurements taken over the range of 472-1150 nm, while the PLE measurements consisted of 980 data points taken over the range from 400-800 nm. To facilitate the point-by-point multiplication, both the visible-light spectra and the PLE data sets were truncated to include only the measurements from 472-800 nm, since this was the largest wavelength interval common to both measurements. This left only 800 data points in the PLE measurements compared to 1642 data points in the spectra measurements. The PLE curves were then resampled using the "resample" command in MATLAB so that both curves consisted of 1642 data points.

After the two curves were multiplied together, the area under the resulting curve was measured by summing all of the pointwise products in SigmaPlot and used to determine a grand total SWIR output. Since not all of the SWIR output

was at wavelengths longer than 1  $\mu\text{m}$ , the total SWIR output was multiplied by the percentage of the phosphor emission that was at wavelengths longer than 1  $\mu\text{m}$ . Both the results for the total SWIR output and the SWIR output at wavelengths greater than 1  $\mu\text{m}$  are in arbitrary units.

Phosphor	Emitter	Total Output (A.U.)	% Output > 1 $\mu\text{m}$	Output > 1 $\mu\text{m}$ (A.U.)
SWIR06	Yellow	73.3	80.3%	58.9
SWIR06	Red	44.4	80.3%	35.7
SWIR07	Yellow	20.8	52.7%	11.0
SWIR07	Red	6.43	52.7%	3.39
SWIR09	Yellow	14.2	82.2%	11.7
SWIR09	Red	11.8	82.2%	9.7

Table 1. Calculated SWIR output from emitter/phosphor combinations, both in terms of total SWIR output and SWIR output at wavelengths greater than 1  $\mu\text{m}$

Of the available emitter/phosphor combinations, the greatest SWIR output resulted from the utilization of the yellow emitter with the thickest SWIR06 sample (B-SWIR06-7S.)

## V. CONCLUSION

### A. VIDEO RECORDING OF SWIR EMISSION

As a final demonstration of the visible-to-SWIR downconversion, a SWIR emitter was constructed using the yellow PLED, the B-SWIR06-7S phosphor, and a 1  $\mu\text{m}$  longpass edge filter. The PLED was powered with series of 6 mA pulses from a Keithley 220 source meter (3 mA per  $\text{cm}^2$ .) The flashing SWIR response was filmed at ranges from 5 m to 100 m in an indoor tunnel at the Night Vision and Electro-Optical Sensor Directorate at Fort Belvoir, Virginia. An InGaAs video camera with an aperture of f/2.0 and a focal length of 200 mm was used for SWIR imagery. The InGaAs camera performed no photo-multiplication or image enhancement. The SWIR emitter was also simultaneously viewed through GEN-III Night Vision Goggles (NVGs).

The flashing SWIR response was plainly visible through the InGaAs camera (Figure 24), but not visible using the NVGs, satisfying the requirement that the SWIR IIFF patch should be undetectable using current-generation night vision devices.



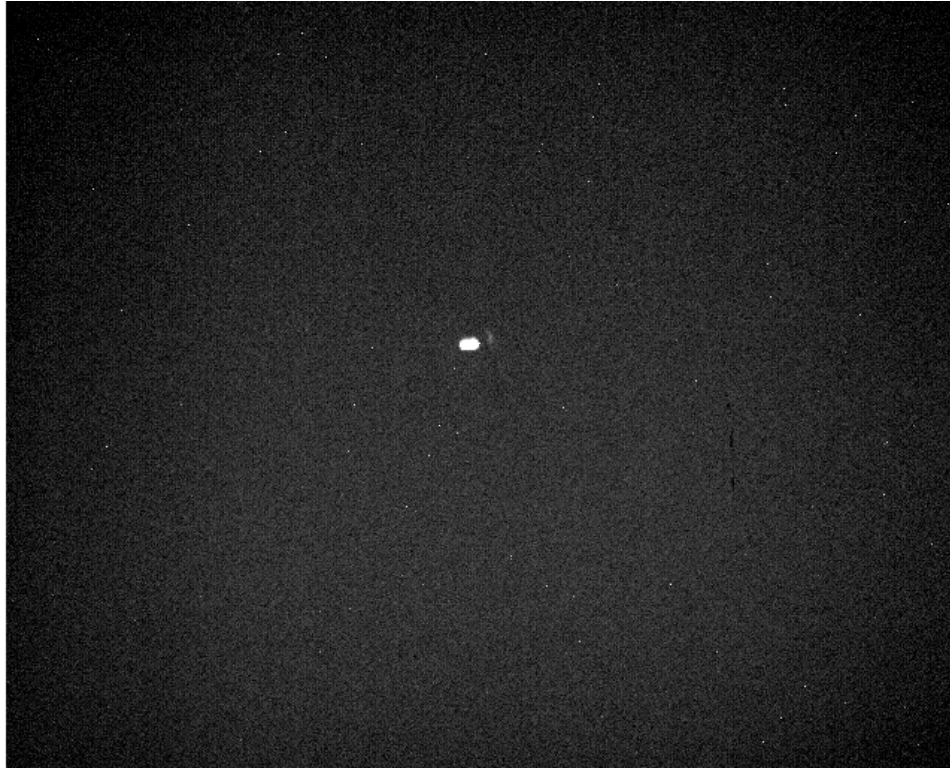


Figure 24. Still frame showing image of SWIR06 phosphor excited with yellow PLED. Recorded with InGaAs camera at a distance of 20 meters.

In addition to the indoor tests, an outdoor test was conducted at a range of 500 m using the same SWIR emitter and InGaAs camera. The SWIR emission was not visible at 500 m, but further investigation indicates that the longpass filters used were not optimized for the application and were likely blocking a significant portion of the emitter's SWIR output at wavelengths shorter than 1200 nm, including the SWIR06 peak near 1.1  $\mu\text{m}$  that accounts for approximately 60% of the phosphor's total SWIR output. The detection experiments (both short- and long-range) should be repeated once the behavior of the longpass filters has been better characterized.

In choosing the optimal combination of PLED, substrate, and phosphor type/thickness, the following were determined: 1) The type of substrate used, as well as the direction of incident illumination, had little effect on the total SWIR output of the device. 2) For all of the phosphors, a thicker pigment layer produced a greater total SWIR output than a thinner layer. 3) The optimum combination measurement to date consists of a 40  $\mu\text{m}$  thick Nd phosphor paste in combination with a yellow PLED emitter.

## **B. FURTHER RESEARCH**

From the tests performed to date on both batches of phosphor samples, it is likely that we have not yet reached the point of diminishing returns in regard to the thickness of the phosphor pigment layer. Further investigation into thicker pigment layers should be of highest priority.

In parallel, research should be performed into the feasibility of eliminating the plastic substrate layer entirely. By mixing the phosphor pigment with a plasticizer and forming the resulting mixture into sheets, it may be possible to produce a self-supporting phosphor structure that would make use of its entire thickness for downconversion, rather than having to utilize a substrate layer that serves no purpose other than to support the phosphor pigment.

Finally, it may be beneficial to investigate a combination of two or more different phosphors in the same sample. By using multiple phosphors that are excited by different visible wavelengths, it may be possible to make use of a greater portion of the visible emission from the

PLED in exciting the phosphor pigments. Phosphor materials emitting at longer wavelengths (e.g., Erbium at 1.54  $\mu\text{m}$ ) should also be investigated.

## LIST OF REFERENCES

- [1] John G. Victor, Matthew C. Wilkinson and Susan Carter. "Screen printing light-emitting polymer patterned devices," *U.S. Patent* No. 6,605,483, August 12, 2003.
- [2] Patrick Williams, "Triggered Infrared Emitter Displays for Individual Identify Friend-or-Foe (IIFF) and Vehicular Mounted Identify Friend-or-Foe (VMIFF) Devices," Naval Postgraduate School, June 2007.
- [3] Product Datasheet, 10SWF-800-B shortpass filter, Newport Corp.
- [4] Dr. Rudiger Paschotta, RP Photonics Consulting, GmbH.
- [5] Md. Abdus Subhan, Takayoshi Suzuki and Sumio Kaizaki. "Stereospecific assembly of chiral -Cr(III)--Ln(III)-oxalato-bridged dinuclear 3d-4f complexes (Ln = Yb or Dy) and near infrared circular dichroism in the 4f-4f transitions," *Dalton Transactions*, 2001, pp. 492-497.
- [6] James Elmore, "Transient Effects of Polymer-Organic Light Emitting Diodes and Their Impact on Individual Identification Friend/Foe (IIFF)," Naval Postgraduate School, December 2008.

THIS PAGE INTENTIONALLY LEFT BLANK

## INITIAL DISTRIBUTION LIST

1. Defense Technical Information Center  
Ft. Belvoir, Virginia
2. Dudley Knox Library  
Naval Postgraduate School  
Monterey, California
3. Professor James H. Luscombe  
Naval Postgraduate School  
Monterey, California
4. Professor Nancy M. Haegel  
Naval Postgraduate School  
Monterey, California
5. Professor Peter P. Crooker  
Naval Postgraduate School  
Monterey, California
6. Lieutenant Commander Scott R. Gardner  
Naval Postgraduate School  
Monterey, California
7. Dr. Devin McKenzie  
Director of Technology  
Add-Vision, Inc.  
Scotts Valley, California
8. Mr. Patrick Williams  
USSOCOM  
Special Operations Acquisition and Logistics Center  
Tampa, Florida
9. LTC Michael Traxler  
USSOCOM  
Special Operations Acquisition and Logistics Center  
Tampa, Florida